

Forensic analysis and differentiation of black powder and black powder substitute chemical signatures by infrared thermal desorption – DART-MS

Thomas P. Forbes* and Jennifer R. Verkouteren

National Institute of Standards and Technology, Materials Measurement Science Division, Gaithersburg, MD, USA.

ABSTRACT: The trace detection and forensic analysis of black powders and black powder substitutes, directly from wipe-based sample collections was demonstrated using infrared thermal desorption (IRTD) coupled with direct analysis in real time mass spectrometry (DART-MS). Discrete 15 s heating ramps were generated, creating a thermal desorption profile that desorbed more volatile species (*e.g.*, organic and semivolatile inorganic compounds) at lower temperatures (250 °C to 400 °C) and nonvolatile inorganic oxidizers at high temperatures (450 °C to 550 °C). Common inorganic components of black powders (*e.g.*, sulfur and potassium nitrate) as well as the alternative and additional organic and inorganic components of common black powder substitutes (*e.g.*, dicyandiamide, ascorbic acid, sodium benzoate, guanidine nitrate, and potassium perchlorate) were detected from polytetrafluoroethylene-coated fiberglass collection wipes with no additional sample preparation. IRTD-DART-MS enabled the direct detection of intact inorganic salt species as nitrate adducts (*e.g.*, $[\text{KClO}_4+\text{NO}_3]^-$) and larger clusters. The larger ion distributions generated by these complex mixtures were differentiated using principal component analysis (PCA) of the mass spectra generated at two points during the thermal desorption profile (low and high temperatures), as well as at high in-source collision induced dissociation (CID). The PCA framework generated by the analysis of two black powders and five black powder substitutes was used to classify samples collected from a commercial firecracker containing both flash powder and black powder. The coupling of IRTD-DART-MS and multivariate statistics demonstrated the powerful utility for detection and discrimination of trace fuel-oxidizer mixtures.

Propellants such as black powder and smokeless powder, along with pyrotechnic mixtures, are among the most abused materials for formulating improvised explosives devices (IEDs) in the United States and internationally. These low explosives consistently rank in annual reviews performed by the Bureau of Alcohol, Tobacco, Firearms and Explosives (ATF) as the most frequently encountered fillers of IEDs, reflecting the availability of these materials.¹ Black powder, which is a classical fuel-oxidizer mixture of potassium nitrate, sulfur, and charcoal, is generally sold as a propellant for primitive-style firearms and incorporated into many pyrotechnic devices. Black powder substitutes (BPS) were introduced in the 1970s to replace black powder and are comprised of different formulations that may include potassium perchlorate or other organic fuels and often exclude sulfur.²⁻⁶ Because BPS were designed to improve upon black powder as a propellant, reduce hazards in manufacture, shipping, and storage, and decrease fouling and odor generation, they have replaced black powder in many commercial applications. Pyrotechnic devices often contain a flash powder, the most common of which is a mixture of potassium perchlorate and aluminum.⁷ As such, potassium nitrate and potassium perchlorate are compounds that may be indicative of the class of low explosives exploited by bomb makers, and screening tools that can detect the presence of these compounds represent a critical need. In addition to screening, forensic analysis of unburned propellants requires identification of the specific black powder, BPS, or pyrotechnic used, which requires detection of components in addition to potassium nitrate and potassium perchlorate. Interest in analytical methods for the detection, identification, and differentiation of these compounds spans both fieldable and laboratory-based techniques.

Fieldable techniques generally focus on high-throughput screening and rapid presumptive analysis applications. These techniques often employ wipe-based collection of particulate from surfaces and, in the case of low explosives, target the characteristic anions from a single compound. For example, ion mobility spectrometry (IMS) targets more volatile species and has demonstrated the detection of sulfur present in black powder and some BPS.^{8,9} IMS typically incorporates a thermal desorber operating at conditions compatible with the wipe and optimized for specific threats,¹⁰ but their maximum temperatures are limited, indicating further improvements would be needed for the detection of the more refractory potassium nitrate and potassium perchlorate. The sulfur component of black powder and a few BPS is also targeted by other fieldable gas-phase detectors such as those based on amplifying fluorescence polymers.¹¹ Likewise, colorimetric tests are popular low cost field techniques, but are limited to the detection, in the case of black powder and BPS, of dissociated NO_3^- and ClO_4^- anions.^{12,13} Detection of these anions has also been demonstrated with portable capillary electrophoresis¹⁴ and fieldable surface enhanced Raman spectroscopy (SERS) platforms.¹⁵

Laboratory-based techniques used in the forensic identification of intact low explosives are summarized in guidelines promulgated by the Technical/Scientific Working Group for Fire and Explosive Analysis (T/SWGFEX) and include 20 different techniques.¹⁶ The guide lists black powder, flash powder, and three BPS as formulations to identify, as well as the components necessary for differentiation. Detection of potassium nitrate is required for identification of black powder; while sulfur and carbon are listed as additional components but not

required for identification. The three BPS require identification of potassium nitrate and at least one other component; potassium perchlorate or ascorbic acid (a class of BPS is based on ascorbic acid as the fuel).^{2, 3, 17} A number of organic fuel components such as sodium benzoate, dicyandiamide (DCD), and 3-nitrobenzoic acid (NBA) are also present in various BPS.^{5, 6} Identification of flash powder is based on the oxidizer, most commonly potassium perchlorate, and the metal fuel. The simultaneous detection of these inorganic and organic components remains a challenge, as does the detection of the intact inorganic oxidizers. Several of the techniques specified by T/SWGFEX have been employed for the characterization of black powders and BPS. Infrared (IR) and Raman spectroscopies, when used in combination, can discriminate among some inorganic oxidizers; less so when the anion is the same and only the cation is different.¹⁸ A range of additional analytical techniques have been used to demonstrate detection of potassium nitrate, potassium perchlorate, and organic fuels, including high-performance liquid chromatography/electrospray ionization quadrupole time-of-flight mass spectrometry (HPLC/ESI-QToFMS),² ion chromatography (IC)/MS,³ gas chromatography (GC)/MS with trimethylsilyl derivatization,⁶ and X-ray powder diffraction (XRPD). In addition, a range of additional mass spectrometry techniques have demonstrated fingerprinting, chemical imaging of spatial distributions, vapor detection, and discrimination of gunpowders, black powder, BPS, and their inorganic oxidizer components. These include secondary ion mass spectrometry (SIMS),¹⁹ atmospheric flow tube (AFT)-MS,²⁰ and laser-based MS techniques.^{21, 22}

As introduced above, the analysis of trace amounts of material collected on wipes is not only utilized by screening techniques, but also for traditional forensic techniques, particularly when available sample is limited. Thermal desorption from wipes can also be used in conjunction with ambient ionization mass spectrometry (MS) platforms such as direct analysis in real time (DART)-MS, exploiting the advantages of rapid analysis and no required sample preparation, common to this class of techniques.^{23, 24} In recent years, DART has become a conventional system used by the forensic science community,^{25, 26} demonstrating wide-ranging detection of explosives,²⁷⁻³³ and exhibiting the potential for field deployment when coupled with portable mass spectrometers.³⁴⁻³⁶ The recent development and progression of infrared thermal desorption (IRTD) of wipe-based collections enables the generation of an inherent temperature ramp during a discrete multi-second infrared emission interval for analyte thermal desorption.^{35, 37} The temperature profiles generated by the IRTD notably enabled the thermal desorption of species at their optimal temperatures, *i.e.*, more volatile species at lower temperatures, while still achieving elevated temperatures necessary for the desorption of refractory inorganic oxidizers. The IRTD platform was coupled with DART-MS and a time-of-flight (TOF) mass analyzer to demonstrate the thermal desorption and detection of nanogram levels of intact nonvolatile inorganic oxidizer salts (*e.g.*, KClO_3 or KClO_4), providing higher fidelity data for detection and discrimination. IRTD-DART-MS has the potential to serve both as a fieldable technique and for laboratory-based analysis of black powder and BPS. It has not only the inherent advantages of rapid analysis coupled with no sample preparation for high throughput but is also capable of detecting both organic and inorganic species necessary for the forensic differentiation of intact powders.

We present the applicability and capabilities of utilizing IRTD-DART-MS in conjunction with principal component analysis (PCA) for the detection and differentiation of black powders and various BPS from wipe-based sample collections. The high fidelity IRTD-DART-MS data and multivariate statistical analysis employed here provided a powerful technique for the differentiation of two black powders and five BPS analytes

EXPERIMENTAL METHODS

Materials. Black powders and black powder substitutes were provided by the Bureau of Alcohol, Tobacco, Firearms & Explosives forensic science laboratory (Ammendale, MD, USA). The present study considered two black powders: (1) Goex Black Powder FFFg† and (2) Elephant Supreme Black Powder FFFg; and five black powder substitutes: (1) Pyrodex RS, (2) Pyrodex P, (3) Triple Seven FFFg, (4) Blackhorn 209, and (5) Jim Shockey's Gold. Powders were analyzed as collected trace solid particulate from sample collection wipes (polytetrafluoroethylene, PTFE-coated fiberglass weave: DSA Detection, LLC, Boston, MA, USA). Solid powder grains were isolated and then crushed with a mortar and pestle. The resulting sample was collected with five individual wipes using a single unidirectional swiping motion. In many cases, the apparent wipe loading was deemed too high (visible dark gray/black deposits) and was reduced by completing a secondary swipe sampling from the original wipe. Wipe-samples from a Super Cobra 6 2G firecracker containing a potassium perchlorate/aluminum flash powder and black powder primer were also analyzed. The firecracker was swiped on the top, bottom, and twice axially along the body. Additional details can be found in the supporting information.

Instrumentation. The IRTD component of the platform was previously described and characterized in detail (Figure S1).^{35, 37} Briefly, the IRTD was comprised of a twin tube near infrared emitter (Heraeus Noblelight America, LLC, Buford, GA, USA), housed within an aluminum casing and capped with a glass-ceramic insulator (Mykroy/Mycalex). The infrared emitter was operated at 100 % power in discrete 15 s emission intervals for each sample. Wipes were inserted directly below the infrared emission focal point. The IRTD unit was coupled to a DART SVP ionization source (IonSense, Saugus, MA, USA) and time-of-flight mass spectrometer (AccuTOF, JEOL USA, Peabody, MA, USA) through a hybrid glass/ceramic/metal junction and Vapur® hydrodynamic-assist interface (operated at 4 L/min) (Figure S1). Negative mode operation demonstrated superior sensitivity for the inorganic salts targeted here and was used throughout. Additional details of this enclosed transport configuration and experimental setup can be found in the literature.^{23, 35} As introduced above, the IRTD-DART-MS platform enables the preservation of intact inorganic salt species (*e.g.*, KClO_4) for robust detection. However, to provide additional confirmation, mass spectra were acquired with a method that switched between orifice 1 voltages of -20 V and -60 V, every 0.5 s. The elevated orifice voltage enabled in-source collision induced dissociation (CID) to induce fragmentation of clusters and adducts, yielding bare anions from inorganic oxidizers (*e.g.*, ClO_4^-) and enhancing their detection.^{21, 31, 38-40} Based on previous work, a -20 V orifice voltage yielded intact organic and inorganic salt species, while -60 V was sufficient to fragment most organics and a significant fraction of inorganic salt species to the bare anion.³⁵ This method enabled acquisition of mass spectra from 1) the beginning of the emission interval –

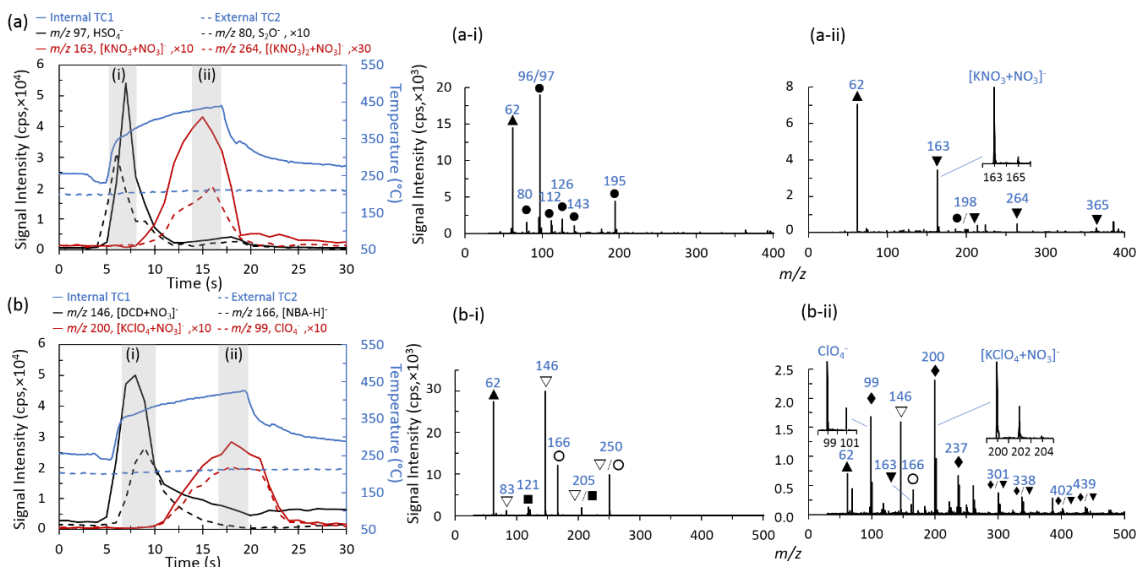


Figure 1. Representative IRTD-DART-MS extracted ion chromatograms (XICs) from (a) Elephant black powder and (b) Triple Seven BPS overlaid with temperature measurements (TC: thermocouple). Corresponding mass spectra from (i) early and (ii) late time points during the emission interval. Presumptive peak identifications found in Table 1.

consisting of the more labile organic and inorganic species, 2) late in the emission interval – consisting of the refractory inorganic oxidizers, and 3) at high in-source CID – yielding bare anions and inorganic species (across early and late timepoints from the desorption profile). Additional DART and MS parameters and settings can be found in the supporting information.

Principal Component Analysis. Principal component analysis (PCA) was employed to reduce the number of variables (in this case mass spectral peaks) to a more manageable set.^{19, 22, 41, 42} Background subtracted (background mass spectra taken from blank wipe control samples) mass spectra were acquired from the raw data at the three sets of conditions listed above. Each extracted mass spectrum consisted of 64,592 data points from m/z 30 to m/z 600. A custom Matlab (Mathworks Inc., Natick, MA, USA) code was developed to read in a series of exported mass spectra files, scale the raw data, and perform PCA, generating scoring and loading values. As described above, given the nature of the sample collection process from particulate powder residues, no effort was made to quantify or equate sample wipe loading across replicates or powders. Therefore, scaling was performed in order to more appropriately compare acquired data across these replicates and samples. The analysis conducted here incorporated pareto scaling, which consisted of mean centered data, divided by the square root of the standard deviation of each variable.⁴³ Unlike autoscaling, which divides mean centered data by the standard deviation, pareto scaling imparts a level of importance to larger variables (mass spectral peaks). PCA scoring and loading plots were generated from five replicate samples for each powder at each of the three conditions described above. These data were used as training data for principal component determinations. The samples collected from a Cobra firecracker containing both flash and black powders were used as testing data.

Safety Considerations. Appropriate safety considerations for the storage and handling of energetic materials were employed per the materials' safety data sheets and in accordance with best practices. Bulk energetic materials should not be exposed to physical, electrical, or thermal insult. A portable fume extractor

was incorporated to protect against any potential aerosol or vapor release of these compounds from the system.

RESULTS AND DISCUSSION

IRTD-DART-MS of Black Powder and BPS. As introduced above and demonstrated in the literature³⁵ and Figure 1, the heating ramp generated by the infrared emission allowed organic and more volatile inorganic species to be thermally desorbed at relatively lower temperatures (Figure 1(i)), while still attaining the elevated temperatures necessary to thermally desorb inorganic oxidizers such as potassium perchlorate and potassium nitrate (Figure 1(ii)). This heating ramp also enabled a level of temporal separation similar to temperature programmed desorption (TPD). Figure 1 demonstrates representative extracted ion chromatograms, IRTD temperature measurements, and associated mass spectra from early and late time points during the emission interval for Elephant black powder and Triple Seven BPS. Details of these temperature measurements and diagrams of the layout can be found in the literature and supporting information.³⁵ Proposed peak assignments were based on literature review, mass and isotopic distribution matching, and previous experience. Peak assignments were labeled by symbols in mass spectra, with corresponding identifications found in Table 1. The Elephant black powder exhibited a range of ions associated with the sulfur and potassium nitrate components. Figure 1 displays the initial desorption and detection of the sulfur component at relatively lower temperatures at the onset of infrared emission, followed by the potassium nitrate oxidizer component as elevated temperatures were reached. The mass spectra corresponding to early in the emission period yielded a range of sulfur-based ions (●), including, m/z 80 S_2O , m/z 96 S_3 , m/z 97 HSO_4^- , m/z 112 S_3O , m/z 126 $S_2NO_3^-$, m/z 143 $[HSO_4^- + NO_2]^-$, and m/z 195 $[H_2SO_4 + HSO_4]^-$ (Figure 1(a-i)).⁸ As temperatures necessary for the thermal desorption of potassium nitrate (▼) were achieved, ions corresponding to the intact inorganic salt were observed in Figure 1(a-ii), specifically, adducts with the available nitrate anions generated by the DART source, the monomer m/z 163 $[KNO_3 + NO_3]^-$, dimer m/z 264 $[(KNO_3)_2 + NO_3]^-$, and trimer m/z 365 $[(KNO_3)_3 + NO_3]^-$. The

Table 1. Main peaks and preliminary assignments observed (✓) for black powder and BPS components.

Major Components	Symbol	MW (g/mol)	Major Ions Observed	<i>m/z</i>	Goex/ Eleph.	Pyro. P / RS	Triple Seven	BH 209	JSG
Potassium Nitrate	▼	101.10	[KNO ₃ +NO ₃] ⁻	163	✓	✓	✓		✓
			[(KNO ₃) ₂ +NO ₃] ⁻	264	✓				
			[(KNO ₃) ₃ +NO ₃] ⁻	365	✓				
Sulfur	●	32.06	S ₂ O ⁻	80	✓	✓			
			S ₃ ⁻	96	✓	✓			
			HSO ₄ ⁻	97	✓	✓			
			S ₃ O ⁻	112	✓				
			S ₂ NO ₃ ⁻	126	✓				
			[HSO ₄ +NO ₂] ⁻	143	✓				
			[H ₂ SO ₄ +HSO ₄] ⁻	195	✓				
			[KNO ₃ +HSO ₄] ⁻	198	✓				
Potassium Perchlorate	◆/▼	138.55	ClO ₄ ⁻	99		✓	✓	✓	✓
			[KClO ₄ +NO ₃] ⁻	200		✓	✓	✓	✓
			[KClO ₄ +ClO ₄] ⁻	237		✓	✓	✓	✓
			[(KNO ₃)(KClO ₄ +NO ₃)] ⁻	301		✓	✓	✓	✓
			[(KNO ₃)(KClO ₄ +ClO ₄)] ⁻	338		✓	✓	✓	✓
			[(KNO ₃) ₂ (KClO ₄ +NO ₃)] ⁻	402		✓	✓	✓	✓
			[(KNO ₃) ₂ (KClO ₄ +ClO ₄)] ⁻	439		✓	✓	✓	✓
			[(KNO ₃) ₂ (KClO ₄) ₂ +NO ₃] ⁻	540					✓
[(KNO ₃) ₂ (KClO ₄) ₂ +ClO ₄] ⁻	577					✓			
Sodium Benzoate	■	144.11	C ₆ H ₅ COO ⁻	121		✓	✓		
Dicyandiamide (DCD)	▽/■	84.08	[DCD-H] ⁻	83		✓	✓		
			[DCD+NO ₃] ⁻	146		✓	✓		
			[DCD+ C ₆ H ₅ COO] ⁻	205		✓	✓		
3-Nitrobenzoic Acid (NBA)	○	167.12	[NBA-H] ⁻	166			✓		
			[NBA+NO ₃] ⁻	229			✓		
			[DCD+NBA-H] ⁻	250				✓	
Ascorbic Acid (AA)	◇	176.12	[AA-H] ⁻	175					✓
			[AA+NO ₃] ⁻	238					✓
			[2AA-H] ⁻	351					✓
Guanidine Nitrate (GN)	□	122.08	[GN+NO ₃] ⁻	184				✓	
			[2GN+NO ₃] ⁻	306				✓	
			[3GN+NO ₃] ⁻	428				✓	
			[4GN+NO ₃] ⁻	550				✓	
Nitrates	▲		NO ₃ ⁻	62	✓	✓	✓	✓	✓
			[HNO ₃ +NO ₃] ⁻	125				✓	✓

ability to detect the intact oxidizer salt provides a more comprehensive presumptive identification and potential differentiation of black powders and BPS. For example, if the potassium nitrate adduct, *m/z* 163 [KNO₃+NO₃]⁻, fragmented down to the bare anion, detection would be confounded by the high abundance of nitrate generated by the DART ionization source and could not be discriminated from other nitrate-based salts, *e.g.*, ammonium nitrate (NH₄NO₃). In a number of cases in this study, adducts between powder components were also observed, for example from Figure 1(a-ii), a sulfur-potassium nitrate adduct, *m/z* 198 [KNO₃+HSO₄]⁻. The Goex black powder demonstrated similar spectra and peak distributions to Elephant black powder (Figure S2). Given the ambient nature of the platform, environmental conditions may alter ionization pathways. However, the mild hygroscopic nature of black powder is not believed to play a major role here. The low level of moisture (likely < 0.5% the composition) would vaporize early in the temperature ramp and not be present during the desorption of the majority of the compounds of interest.

Figure 1(b) demonstrates a similar analysis for the BPS, Triple Seven. As introduced above, BPS were developed to provide enhanced performance and reduced corrosion and odor

generations. The Triple Seven composition eliminated the sulfur component and was comprised of potassium nitrate (PN), charcoal, potassium perchlorate (PPC), sodium benzoate, dicyandiamide (DCD), dextrin, and 3-nitrobenzoic acid (NBA).⁶ Early in the infrared emission interval, desorption and detection of the organic species were observed, including the benzoate anion (■): *m/z* 121 C₆H₅COO⁻, the deprotonated and nitrate adduct of dicyandiamide (▽): *m/z* 83 [DCD-H]⁻ and *m/z* 146[DCD+NO₃]⁻, deprotonated nitrobenzoic acid (○): *m/z* 166 [NBA-H]⁻, and adducts *m/z* 205 [DCD+ C₆H₅COO]⁻ and *m/z* 250 [DCD+NBA-H]⁻ (Figure 1(b-i)). The IRTD platform achieved temperatures necessary for the thermal desorption of the refractory potassium perchlorate salt. Previous work demonstrated incomplete desorption of the non-volatile potassium chlorate and perchlorate salts within the 15 s emission interval, limited by the thermal properties of the wipe material. However, sufficient material was desorbed for 5 ng to 10 ng sensitivities from the individual salts.³⁵ Figure 1(b-ii) displays the ion distribution observed at elevated temperatures achieved late in the emission interval. The distribution was dominated by the intact potassium perchlorate nitrate adduct (◆), *m/z* 200 [KClO₄+NO₃]⁻, and bare perchlorate anion, *m/z* 99 ClO₄⁻,

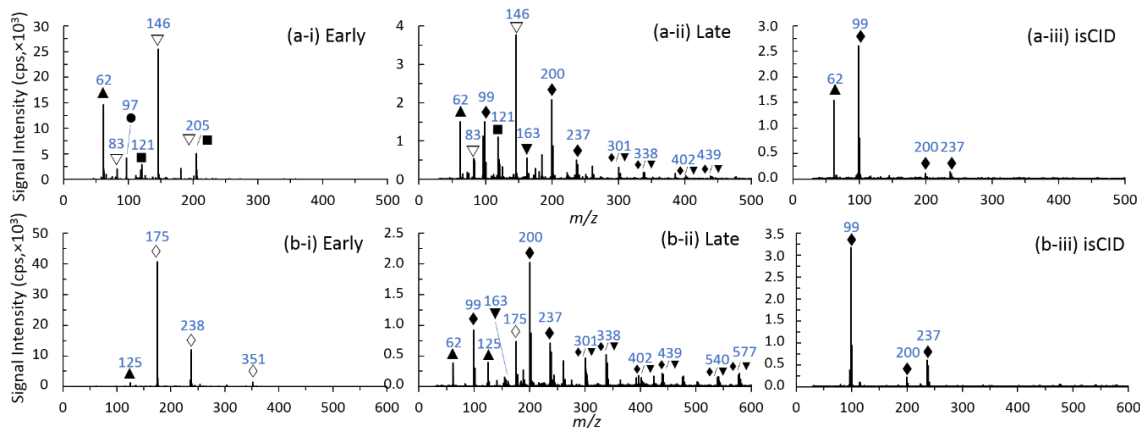


Figure 2. Representative IRTD-DART-MS mass spectra of (a) Pyrodex RS BPS and (b) Jim Shockey's Gold BPS from (i) early and (ii) late time points during the emission interval and (iii) at high in-source collision induced dissociation. Presumptive peak identifications found in Table 1.

although various adducts (*e.g.*, m/z 237 [$\text{KClO}_4+\text{ClO}_4$]) and clusters with potassium nitrate (*e.g.*, m/z 301 [$(\text{KNO}_3)(\text{KClO}_4)+\text{NO}_3$]) were also observed (Figure 1(b-ii) and Table 1). Prior investigations into individual chlorate and perchlorate salt samples demonstrated adduct formation with available nitrate (generated by the DART source) or free anions from the sample were the dominant ions formed.³⁵ Dissociation and/or recombination of cation-anion pairs remains a function of the original salt properties. The ability of IRTD-DART-MS to provide direct information to the composition of intact salt species provides an additional level of information from mass spectra. Alternative mass spectrometry techniques such as GC/MS traditionally do not achieve temperatures sufficient to vaporize and detect inorganic compounds (*i.e.*, potassium nitrate or potassium perchlorate). Similarly, liquid-based mass spectrometry techniques, including LC/MS and ESI-MS, require the dissolution of the analyte in solvent, losing the intact salt information that IRTD-DART-MS enables.

In addition to the separation and potential differentiation of black powder and BPS by the temporal distribution of chemical species (Figure 1), we also utilized in-source CID to target fragmentation and declustering of the larger inorganic adducts and clusters generated by IRTD-DART-MS. Figure 2 displays representative mass spectra from both early and late in the thermal desorption profile, as well as at high in-source CID for the Pyrodex RS and Jim Shockey's Gold BPS. Many of the BPS considered here contained both potassium perchlorate and potassium nitrate, yielding a large ion distribution containing numerous adducts and clusters of the two (Figure 1(b), Figure 2, and Table 1). By applying an elevated potential to orifice 1, increased fragmentation of these clusters was achieved. Figure 2(iii) demonstrates the high in-source CID spectra for Pyrodex RS and Jim Shockey's Gold, clearly identifying the perchlorate anion representative of the potassium perchlorate component. Though high in-source CID improves the detection of the bare anions, peaks associated with the intact salts were significantly reduced or eliminated at these settings.

Further consideration of the spectra for these BPS provided points of differentiation with alternative powders. As demonstrated in Figure 1(a), the black powders yielded strong peaks for a wide range of sulfur ions, as well as potassium nitrate adducts with nitrate. The Pyrodex RS and P black powder

substitutes contained reduced levels of sulfur and potassium nitrate, while adding potassium perchlorate, sodium benzoate and dicyandiamide. A number of the main sulfur related ions and the potassium nitrate were still observed, along with peaks associated with the remaining compounds (Figure 2(a)). Pyrodex was the only BPS to contain sulfur, providing a point of differentiation. In addition, as compared to the similar composition of Triple Seven BPS, the presence or absence of sulfur and 3-nitrobenzoic acid (m/z 166 [NBA-H^-]) enabled differentiation. Jim Shockey's Gold BPS is based on ascorbic acid and was unique in that regard in this sample set, enabling clear differentiation (Figure 2(b)). Jim Shockey's Gold BPS consisted of potassium nitrate, potassium perchlorate, and ascorbic acid (\diamond), observed as both the deprotonated anion, m/z 175 [AA-H^-], and the nitrate adduct, m/z 238 [$\text{AA}+\text{NO}_3$].³ The precise composition of Blackhorn 209 BPS was proprietary, with only general ingredient classes provided by the manufacturer. Related patents and the literature indicated it contains nitrocellulose, guanidine nitrate, and potassium perchlorate.^{5, 20} However, prior analysis has also demonstrated that Blackhorn 209 was comprised of a mixture of particles, some containing potassium perchlorate and some containing potassium nitrate.⁴⁴ No readily identifiable peaks associated with nitrocellulose were observed here, however, an array of guanidine nitrate adducts (\square) (*e.g.*, m/z 184 [$(\text{C}(\text{NH}_2)_3\text{NO}_3)+\text{NO}_3$] and m/z 306 [$(\text{C}(\text{NH}_2)_3\text{NO}_3)_2+\text{NO}_3$]) and potassium perchlorate enabled differentiation from the other powders investigated here (Figure S3).

Principal Component Analysis of Black Powder and BPS.

The detection, presumptive mass spectral peak identification, and possibilities for differentiation of black powder and BPS was introduced above. However, given the complex nature of these multi-component mixtures, large ion distributions were observed, which can lead to difficulties with differentiation. Here, we employed principal component analysis of the complete powder signature as an alternative to targeting specific species for identification and differentiation. PCA was conducted at each of the three sets of conditions described above. Details of the analysis and incorporated scaling can be found in the Experimental Methods section. Figure 3 displays the scores plot for the first three principal components from the analysis of mass spectra taken early during the thermal desorption profile at low in-source CID (Figure S4 – 2D projections of first

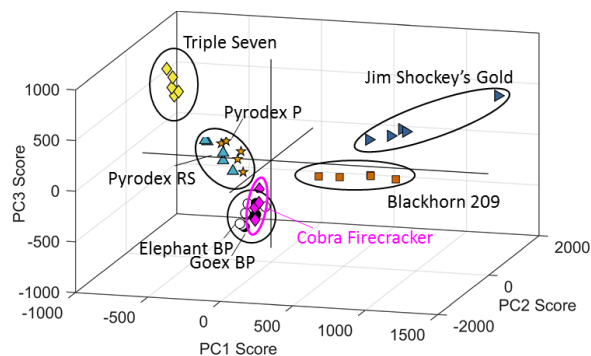


Figure 3. Principal component analysis scores plot of the mass spectral signatures early in the infrared emission interval – relatively low desorption temperatures. Plot displays the first three principal components for training data: Elephant (○) and Goex (●) black powders, and Triple Seven (◆), Pyrodex RS (▲), Pyrodex P (★), Blackhorn 209 (■), and Jim Shockey's Gold (▶) BPS; and testing data: Cobra firecracker (◆).

two components for easier visualization). As demonstrated, the PCA results provided differentiation of the powders investigated here. The two black powders were comprised of very similar formulations and clustered together as expected. Similarly, the Pyrodex P and Pyrodex RS BPS were clustered together as expected given their identical composition with differences only in grain size, an aspect not expected to directly affect the chemical detection for the analysis here. Microscopy-based inspection would be necessary for their differentiation. The remaining three BPS, Triple Seven, Blackhorn 209, and Jim Shockey's Gold were all readily separated and independently clustered.

The PCA loading plots for the first three principal components, shown in Figure 4, further identified the compounds and peaks providing discrimination of the black powders and BPS based on this analysis. The first principal component drove the differentiation of the Blackhorn and Jim Shockey's Gold BPS (positive PC1 score) from the Triple Seven BPS (negative PC1 score), with the Pyrodex BPS and Goex/Elephant black powders all falling near the axis (Figure 3 and Figure S4). The differentiation was dominated by the ascorbic acid of Jim Shockey's Gold and guanidine nitrate of Blackhorn (both positive PC1 scores) versus the dicyandiamide and 3-nitrobenzoic acid of Triple Seven (negative PC1 scores Figure 4(a)). Other minor contributions from sulfur-related ions yielded negative PC1 loadings and resulted in the black powders falling near the axis and just negative in the PCA scores plot (Figure 3 and S4). The second principal component (PC2 – Figure 4(b)) almost exclusively differentiated between the ascorbic acid of Jim Shockey's Gold relative to the guanidine nitrate of Blackhorn BPS. The remaining BPS (Triple Seven and Pyrodex RS/P) and black powders (Goex and Elephant) fell along the axis with minimal PC2 loadings. The third principal component (PC3) yielded positive loadings for the dicyandiamide and 3-nitrobenzoic acid components of the Triple Seven BPS, with additional peaks representative of ascorbic acid and benzoate, relative to negative loadings dominated by sulfur related ions. This enabled clear differentiation of the black powders from the remaining BPS, most notably Triple Seven. The Pyrodex BPS fell along the axis as they contained sodium benzoate and dicyandiamide (positive PC3 loadings) and sulfur (negative PC3 loadings).

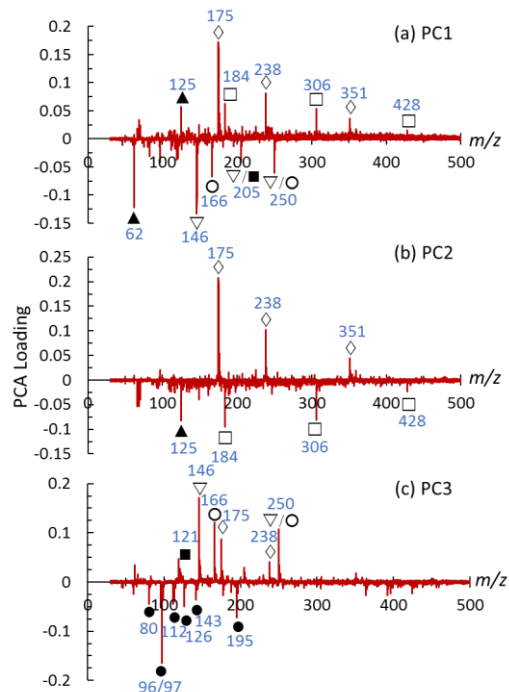


Figure 4. Principal component analysis loading plots of the mass spectral signatures early in the infrared emission interval for (a)–(c) the first three principal components.

Principal component analyses were also conducted on the mass spectra collected for each sample late in the thermal desorption profile (at elevated temperatures) and at high in-source CID. Figure 5 displays the PCA scores plots of the first three principal components for these two additional cases. As introduced above in the detailed discussion of the ion distributions generated by the black powders and BPS, the inorganic salts were observed at higher temperatures (Figure 1(ii) and 2(ii)). Similarly, fragmentation of the larger inorganic salt clusters and adducts was observed at high in-source CID (Figure 2(iii)). The principal components for both these settings separated the black powders from the majority of the BPS, excluding Blackhorn 209. The PCA loadings plot for the powder signatures at elevated temperatures demonstrated PC1 separation based on the presence of dicyandiamide and potassium nitrate versus typical background peaks observed for Blackhorn 209 samples (Figure 5(a) and S5(a)). Beyond very minimal potassium perchlorate and typical background peaks, the Blackhorn BPS exhibited no other distinct compound specific peaks at elevated temperatures. The dicyandiamide-related ions demonstrated long trailing peaks in the extracted ion chromatograms (Figure 1(b)) that remained late into the infrared emission interval. The black powders and majority of BPS all contained potassium nitrate, resulting in the clear differentiation from Blackhorn 209, which did not. The second principal component for the high temperature signatures differentiated between those signals dominated by potassium nitrate (the black powders) and those dominated by potassium perchlorate (the remaining BPS) (Figure 5(a) and S5(b)). The third principal component exhibited separation based on again dicyandiamide and benzoate (positive PC3) versus potassium perchlorate dominated ion distribution (negative PC3). Further principal components provided separation based on the remnants of organic peaks that were better differentiated

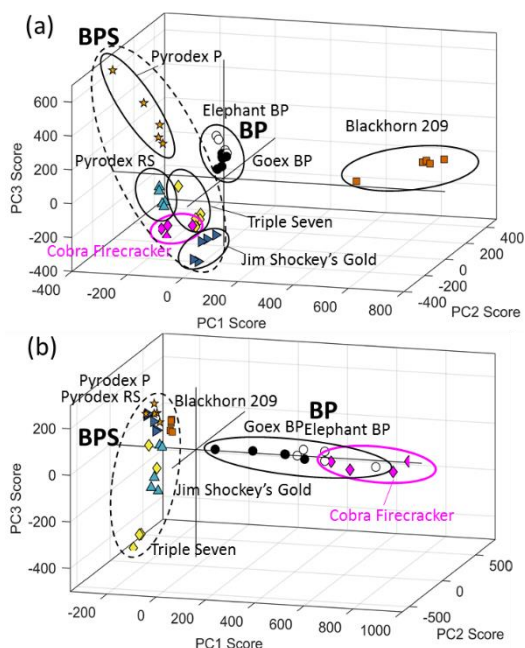


Figure 5. Principal component analysis scores plots of the mass spectral signatures (a) late in the infrared emission interval and (b) at high in-source collision induced dissociation. Plot displays the first three principal components for training and testing data as labeled in Figure 3.

by the lower temperature spectra in Figure 3. The first principal component for the mass spectra at high in-source CID separated the powders between those dominated by sulfur fragments (black powders) and those dominated by nitrate and perchlorate anions (BPS) (Figure 5(b) and S6). These were the main constituents that survived at higher in-source CID. The second principal component then differentiated those BPS with significant perchlorate signal versus those demonstrating nitrate and guanidine nitrate (Blackhorn 209). This provided isolation of the Blackhorn 209 and separation from the other BPS and black powders (Figure S4(c)). Further principal components provided little additional differentiation.

Finally, the principal component analysis demonstrated here was utilized to classify a test example. In this scenario, the previous samples were defined as the training data, which determined the principal components. The corresponding principal components were then calculated for the test case mass spectra. Here, four samples were collected from the outside of a firecracker container known to contain flash powder (comprised of potassium perchlorate and aluminum) and a black powder primer and analyzed by IRTD-DART-MS (Figure S7). This example provided an interesting test as the sample was expected to contain the typical components of a black powder, with the addition of potassium perchlorate common to BPS. However, none of the alternative and additional components of BPS identified here were present. The PCA results for the Cobra firecracker were overlaid onto Figures 3 and 5, demonstrating the scores plots for early and late in the emission interval, as well as at high in-source CID. As might be expected, the mass spectra early in the infrared emission period were dominated by the sulfur species, which led to PCA scores representative of the black powder component of the firecracker, falling near the

Goex and Elephant black powders (Figure 3, see Figure S4 for 2D representations). However, at the elevated temperatures late in the emission interval, the firecracker sample exhibited both the potassium nitrate of the black powder primer and the potassium perchlorate of the flash powder (Figure 5 and S4). The strong potassium perchlorate signal led to strong negative PC2 scores for the “late” settings, falling more in-line with the BPS. At high in-source CID, the Cobra firecracker still exhibited a sulfur peak distribution, yielding a high positive PC1 value, in line with the black powders. However, the perchlorate signal at high in-source CID led to a strong negative PC2 score, providing clear differentiation from the black powder, toward the BPS (Figure S4(c)). This unique example demonstrated how the incorporation of a heating ramp and analysis of spectra at multiple points, as well as at multiple in-source CID levels enabled the differentiation of a mixed composition. If only the relatively lower temperature thermal desorption had been used (Figure 3) or detection based on a single component (*e.g.*, sulfur), the firecracker sample would have been mistakenly classified as a black powder. Achieving the elevated temperatures necessary for the thermal desorption of nonvolatile inorganic oxidizers enabled the firecracker to be differentiated from both black powders and BPS, while exhibiting similarities with both. It is important to note that real world samples may include a wide range of additional components, supplemental fuels or oxidizers, binders, or colorants. Generating a more encompassing training data set will be imperative to providing accurate differentiation of these samples. Similarly, the analysis of post-blast debris or other forensically relevant samples may also include significant background from the device materials or environment that must be considered.

CONCLUSIONS

The IRTD-DART-MS coupling was utilized here for the detection and differentiation of fuel-oxidizer mixtures directly from wipe-based collections, including two black powders, five black powder substitutes, and a flash powder. Principal component analysis at multiple locations in the thermal desorption profile and at high in-source CID enabled the discrimination of these powders based on an array of components and associated ions. The infrared emission generated a rapid heating ramp for the thermal desorption of organic and refractory nonvolatile inorganic components. Traditional methods for the detection of these fuel-oxidizer mixtures require lengthy extractions and separations or only target individual components, providing less robust differentiation. The described platform enabled rapid analysis (15 s) with no sample preparation and generated high fidelity mass spectra for presumptive identification and discrimination. Contrary to most analytical techniques available for the analysis of inorganic oxidizers, the IRTD-DART-MS platform maintained and detected the intact salts, as opposed to solely the bare anion. In addition, no significant decomposition or degradation of the organic components of the investigated black powder substitutes was observed.

This analysis of fuel-oxidizer mixtures also revealed limitations of the currently used wipe material for highly loaded sample collections. Heavily loaded wipes were observed to degrade and melt at temperatures lower than previously demonstrated for the analysis of solely inorganic oxidizers.³⁵ As introduced above, this was circumvented by secondary wiping of initially highly loaded samples to reduce overall loading. This reinforces

the need for an alternative wipe material exhibiting resistance to elevated temperatures, as well as the necessary absorption spectra characterized in our previous work (*i.e.*, transmission of the infrared energy to the glass-mica bottom plate).³⁵ Recent patents have introduced alternative wipe options incorporating phenyl silane coatings intended for elevated temperatures that might be considered.^{45, 46} Alternatively, metallic cloth or mesh materials might provide the necessary infrared radiation transmission characteristics and heat resistance to reduce wipe degradation from deflagrating fuel-oxidizer sample collections. Despite these limitations, the IRTD-DART-MS platform combined with multivariate statistics demonstrated unique capabilities and potential as a forensic analysis tool for the detection and differentiation of fuel-oxidizer mixtures. In addition, previous demonstration of IRTD-DART coupled with a single quadrupole mass analyzer³⁵ has opened possible avenues for field deployment of this platform as well as conceivable opportunities for coupling with IMS or other detection schemes. However, common fieldable techniques often yield poorer resolution and specificity relative to the laboratory mass spectrometer used here. The employed PCA method would need to be revalidated or an alternative detection algorithm developed.

ASSOCIATED CONTENT

Supporting Information

Additional parameters, settings, mass spectra, and figures as noted in the text can be found in the online version.

AUTHOR INFORMATION

Corresponding Author

* E-mail: thomas.forbes@nist.gov.

Notes

† Certain commercial equipment, instruments, or materials are identified in this paper in order to specify the experimental procedure adequately. Such identification is not intended to imply recommendation or endorsement by NIST, nor is it intended to imply that the materials or equipment identified are necessarily the best available for the purpose.

‡ Official contribution of the National Institute of Standards and Technology; not subject to copyright in the United States.

ACKNOWLEDGMENT

The authors would like to thank Cindy Wallace at the Bureau of Alcohol, Tobacco, Firearms, and Explosives for providing the black powders and black powder substitutes, as well as Karlijn Bezemer and Arian van Asten at the Netherland Forensic Institute for providing the firecracker test samples.

REFERENCES

- United States Bomb Data Center (USBDC) Explosives Incident Report (EIR). <https://www.atf.gov/resource-center/data-statistics>, August 15, 2018.
- Bottegali, M.; Lang, L.; Miller, M.; McCord, B., *Rapid Commun. Mass Spectrom.*, **2010**, *24*, 1377-1386.
- Lang Gui-hua, L.; Boyle, K. M., *J. Forensic Sci.*, **2009**, *54*, 1315-1322.
- Pawlak, D. E.; Levenson, M. Deflagrating propellant compositions. U.S. Patent No. 4,128,443, 1978.
- Racette, M.; Viau, S.; Lepage, D. Black powder substitutes for small caliber firearms. US Patent No. 8,257,522, 2012.
- Routon, B. J.; Kocher, B. B.; Goodpaster, J. V., *J. Forensic Sci.*, **2011**, *56*, 194-199.
- Martín-Alberca, C.; García-Ruiz, C., *TrAC-Trend. Anal. Chem.*, **2014**, *56*, 27-36.
- Crawford, C. L.; Boudries, H.; Reda, R. J.; Roscioli, K. M.; Kaplan, K. A.; Siems, W. F.; Hill, H. H., *Anal. Chem.*, **2010**, *82*, 387-393.
- Liang, X.; Zhou, Q.; Wang, W.; Wang, X.; Chen, W.; Chen, C.; Li, Y.; Hou, K.; Li, J.; Li, H., *Anal. Chem.*, **2013**, *85*, 4849-4852.
- Najarro, M.; Davila Morris, M. E.; Staymates, M. E.; Fletcher, R.; Gillen, G., *Analyst*, **2012**, *137*, 2614-2622.
- Cumming, C., *Trace Chemical Sensing of Explosives: "Explosives detection based on amplifying fluorescence polymers"*. John Wiley & Sons, Inc.: Hoboken, New Jersey, USA, 2007, p 195-209.
- Peters, K. L.; Corbin, I.; Kaufman, L. M.; Zreib, K.; Blanes, L.; McCord, B. R., *Anal. Methods*, **2015**, *7*, 63-70.
- Chabaud, K. R.; Thomas, J. L.; Torres, M. N.; Oliveira, S.; McCord, B. R., *Forensic Chem.*, **2018**, *9*, 35-41.
- Hutchinson, J. P.; Evenhuis, C. J.; Johns, C.; Kazarian, A. A.; Breadmore, M. C.; Macka, M.; Hilder, E. F.; Guijt, R. M.; Dicoski, G. W.; Haddad, P. R., *Anal. Chem.*, **2007**, *79*, 7005-7013.
- Chen, J.; Shi, Y.-e.; Zhang, M.; Zhan, J., *RSC Adv.*, **2016**, *6*, 51823-51829.
- Recommended Guidelines for Forensic Identification of Intact Explosives. <https://www.swgfox.com/publications>, August 15, 2018.
- Wehrli, P. A. Explosive and propellant composition and method. US Patent 4,997,496, 1991.
- Zapata, F.; García-Ruiz, C., *Spectrochim. Acta A.*, **2018**, *189*, 535-542.
- Mahoney, C. M.; Gillen, G.; Fahey, A. J., *Forensic Sci. Int.*, **2006**, *158*, 39-51.
- Ewing, R. G.; Valenzuela, B. R.; Atkinson, D. A.; Wilcox Freeburg, E. D., *Anal. Chem.*, **2018**.
- Forbes, T. P.; Sisco, E., *Anal. Chim. Acta*, **2015**, *892*, 1-9.
- Flanigan, P. M.; Brady, J. J.; Judge, E. J.; Levis, R. J., *Anal. Chem.*, **2011**, *83*, 7115-7122.
- Sisco, E.; Forbes, T. P.; Staymates, M. E.; Gillen, G., *Anal. Methods*, **2016**, *8*, 6494-6499.
- Sisco, E.; Verkouteren, J.; Staymates, J.; Lawrence, J., *Forensic Chem.*, **2017**, *4*, 108-115.
- Laramée, J. A.; Cody, R. B.; Nilles, J. M.; Durst, H. D., *Forensic Application of DART (Direct Analysis in Real Time) Mass Spectrometry*. In *Forensic Analysis on the Cutting Edge*, John Wiley & Sons, Inc.: 2007; pp 175-195.
- Pavlovich, M. J.; Musselman, B.; Hall, A. B., *Mass Spectrom. Rev.*, **2016**, DOI: 10.1002/mas.21509.
- Sisco, E.; Dake, J.; Bridge, C., *Forensic Sci. Int.*, **2013**, *232*, 160-168.
- Forbes, T. P.; Sisco, E., *Anal. Methods*, **2015**, *7*, 3632-3636.
- Nilles, J. M.; Connell, T. R.; Stokes, S. T.; Dupont Durst, H., *Propell., Explos., Pyrot.*, **2010**, *35*, 446-451.
- Forbes, T. P.; Sisco, E., *Analyst*, **2018**, *143*, 1948-1969.
- Forbes, T. P.; Sisco, E.; Staymates, M.; Gillen, G., *Anal. Methods*, **2017**, *9*, 4988-4996.
- Sisco, E.; Forbes, T. P., *Analyst*, **2015**, *140*, 2785-2796.
- Clemons, K.; Dake, J.; Sisco, E.; Verbeck, G. F., *Forensic Sci. Int.*, **2013**, *231*, 98-101.
- Bernier, M. C.; Li, F.; Musselman, B.; Newton, P. N.; Fernández, F. M., *Anal. Methods*, **2016**, *8*, 6616-6624.
- Forbes, T. P.; Sisco, E.; Staymates, M., *Anal. Chem.*, **2018**, *90*, 6419-6425.
- Gómez-Ríos, G. A.; Vasiljevic, T.; Gionfriddo, E.; Yu, M.; Pawliszyn, J., *Analyst*, **2017**, *142*, 2928-2935.
- Forbes, T. P.; Staymates, M.; Sisco, E., *Analyst*, **2017**, *142*, 3002-3010.
- Evans-Nguyen, K. M.; Gerling, J.; Brown, H.; Miranda, M.; Windom, A.; Speer, J., *Analyst*, **2016**, *141*, 3811-3820.
- Evans-Nguyen, K. M.; Quinto, A.; Hargraves, T.; Brown, H.; Speer, J.; Glatter, D., *Anal. Chem.*, **2013**, *85*, 11826-11834.
- Forbes, T. P.; Sisco, E., *Anal. Chem.*, **2014**, *86*, 7788-7797.
- Perez, J. J.; Flanigan, P. M.; Brady, J. J.; Levis, R. J., *Anal. Chem.*, **2012**, *85*, 296-302.
- Wagner, M. S.; Castner, D. G., *Langmuir*, **2001**, *17*, 4649-4660.
- van den Berg, R. A.; Hoefsloot, H. C.; Westerhuis, J. A.; Smilde, A. K.; van der Werf, M. J., *BMC Genomics*, **2006**, *7*, 142.
- Lang, G. L.; Reis, K. In *Characterization and Analysis of Blackhorn 209, a New Black Powder Substitute*, America Academy of

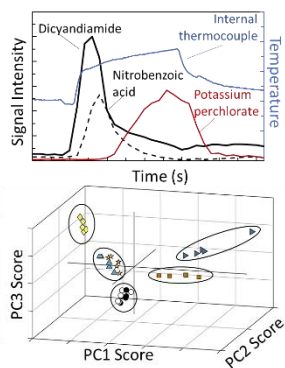
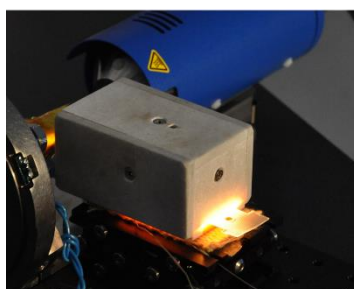
Forensic Sciences Annual Scientific Meeting, Seattle, WA, February 22-27, 2010; Seattle, WA, 2010.

(45) Addleman, R. S.; Atkinson, D. A.; Bays, J. T.; Chouyyok, W.; Cinson, A. D.; Ewing, R. G.; Gerasimenko, A. A. Enhanced surface sampler and process for collection and release of analytes. US8943910 B2, 2015.

(46) Addleman, R. S.; Li, X. S.; Chouyyok, W.; Atkinson, D. A. Collection, release, and detection of analytes with polymer composite sampling materials. US20160313218 A1, 2015.

Insert Table of Contents artwork here

IRTD-DART-MS



Supporting Information for: Forensic analysis and differentiation of black powder and black powder substitute chemical signatures by infrared thermal desorption – DART-MS

Thomas P. Forbes* and Jennifer R. Verkouteren

National Institute of Standards and Technology, Materials Measurement Science Division, Gaithersburg, MD, USA

* Corresponding author: E-mail: thomas.forbes@nist.gov; Tel: 1-301-975-2111

Supporting Information Table of Contents

Experimental Methods

Materials.

Temperature measurements.

Supplemental Tables, Mass Spectra, and Figures

Table S1. System parameters and settings.

Figure S1. Schematic representation of the IRTD-DART-MS platform

Figure S2. Representative mass spectra of Goex black powder

Figure S3. Representative mass spectra of Blackhorn 209 black powder substitute

Figure S4. 2D representations of PCA scores plots for first three principal components from mass spectra acquired early and late in the emission period and at high in-source CID.

Figure S5. PCA loading plots for late in the emission period

Figure S6. PCA loading plots for high in-source CID

Figure S7. Representative mass spectra of Cobra firecracker

Experimental Methods

Materials.

Black powders: (1) Goex Black Powder FFFg (Goex Powder, Inc. Doyline, Louisiana, USA), and (2) Elephant Supreme Black Powder FFFg.

Black powder substitutes: (1) Pyrodex RS (Hodgdon Powder Company, Shawnee, KS, USA), (2) Pyrodex P (Hodgdon Powder Company), (3) Triple Seven FFFg (Hodgdon Powder Company), (4) Blackhorn 209 (Western Powders, Inc., Miles City, MT, USA), and (5) Jim Shockey's Gold (American Pioneer Powder, Inc., Boca Raton, FL, USA).

Temperature measurements. Two thermocouples (TC) on the bottom plate of the IRTD housing provided real-time temperature measurements. The internal thermocouple (TC1) provided temperature data of the bottom plate directly below the infrared emission point and the external thermocouple (TC2) from the opposite side of the bottom plate.

Supplemental Tables, Mass Spectra, and Figures

Table S1. DART-MS parameters and settings.

<i>DART Source Parameters</i>			
DART gas	N ₂	DART gas temperature	400 °C
DART grid voltage	100 V	Vapor flow rate	4 L/min
<i>AccuTOF Parameters</i>			
Orifice 1 voltage	-20 V and -60 V	Orifice 2 voltage	-5 V
Ring lens voltage	-5 V	Peaks voltage	-400 V
Detector voltage	-2300 V	Orifice temperature	100 °C

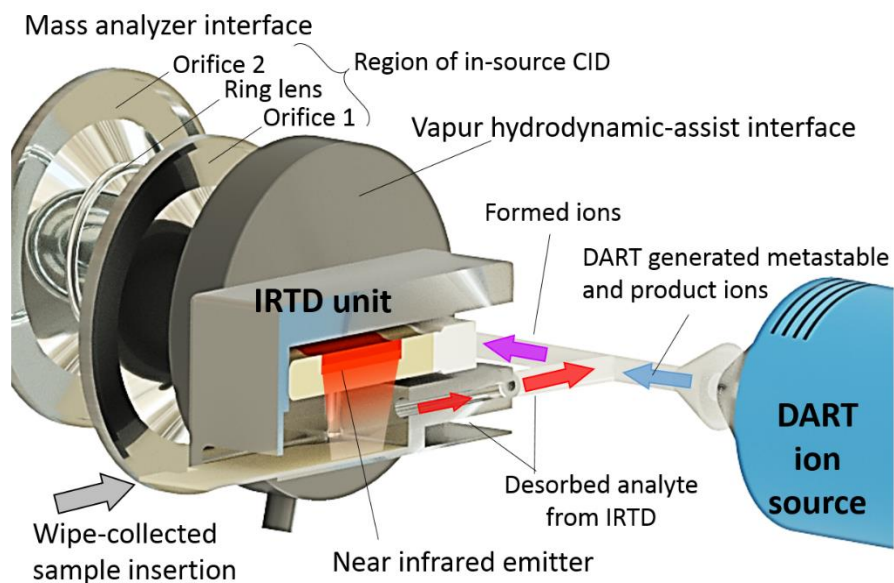


Figure S1. Schematic representation of the IRTD-DART-MS analysis of wipe-based sample collections. The twin tube near infrared emitter was located within an aluminum enclosure that enabled wipe introduction for exposure. Vaporized samples were entrained into the T-junction and ionized by DART generated metastable and product ion species. Ions pulled into the mass spectrometer were declustered by in-source collision induced dissociation between orifice 1 and the ring lens.

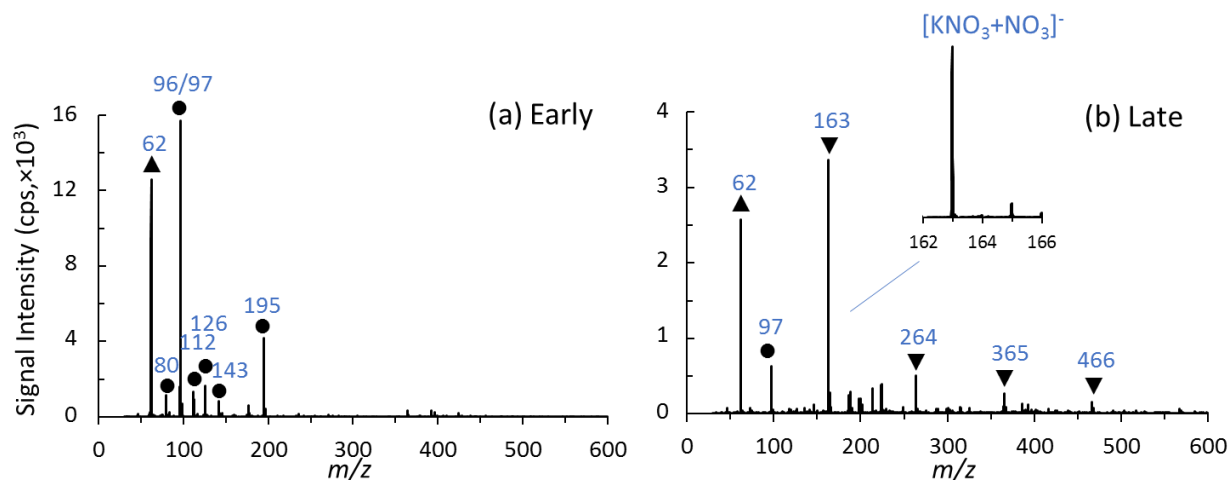


Figure S2. Representative mass spectra of Goex black powder from (a) early and (b) late time points during the emission interval. Presumptive peak identifications found in Table 1.

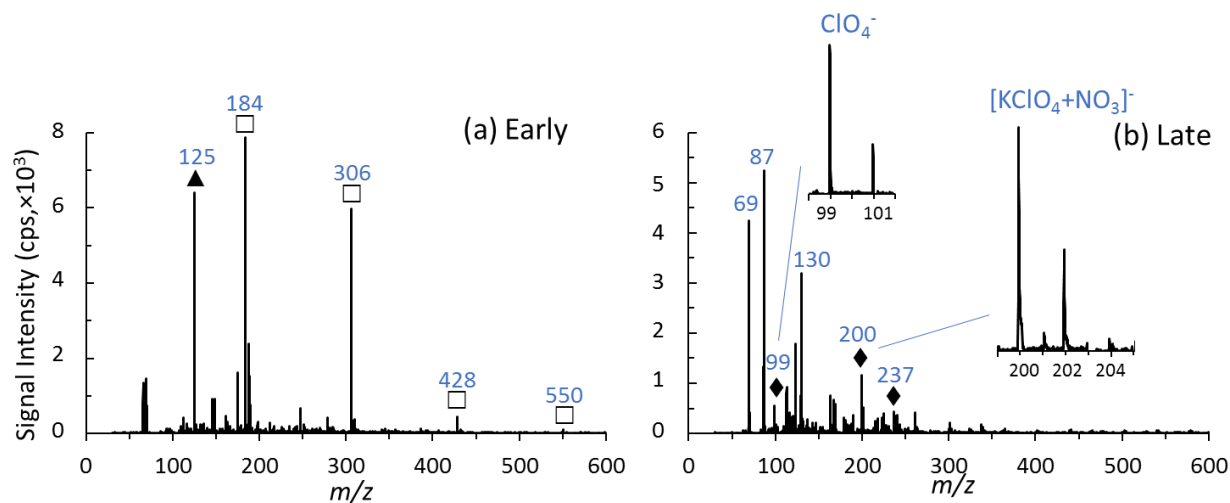


Figure S3. Representative mass spectra of Blackhorn 209 BPS from early in the emission interval (relatively low temperatures). Presumptive peak identifications found in Table 1.

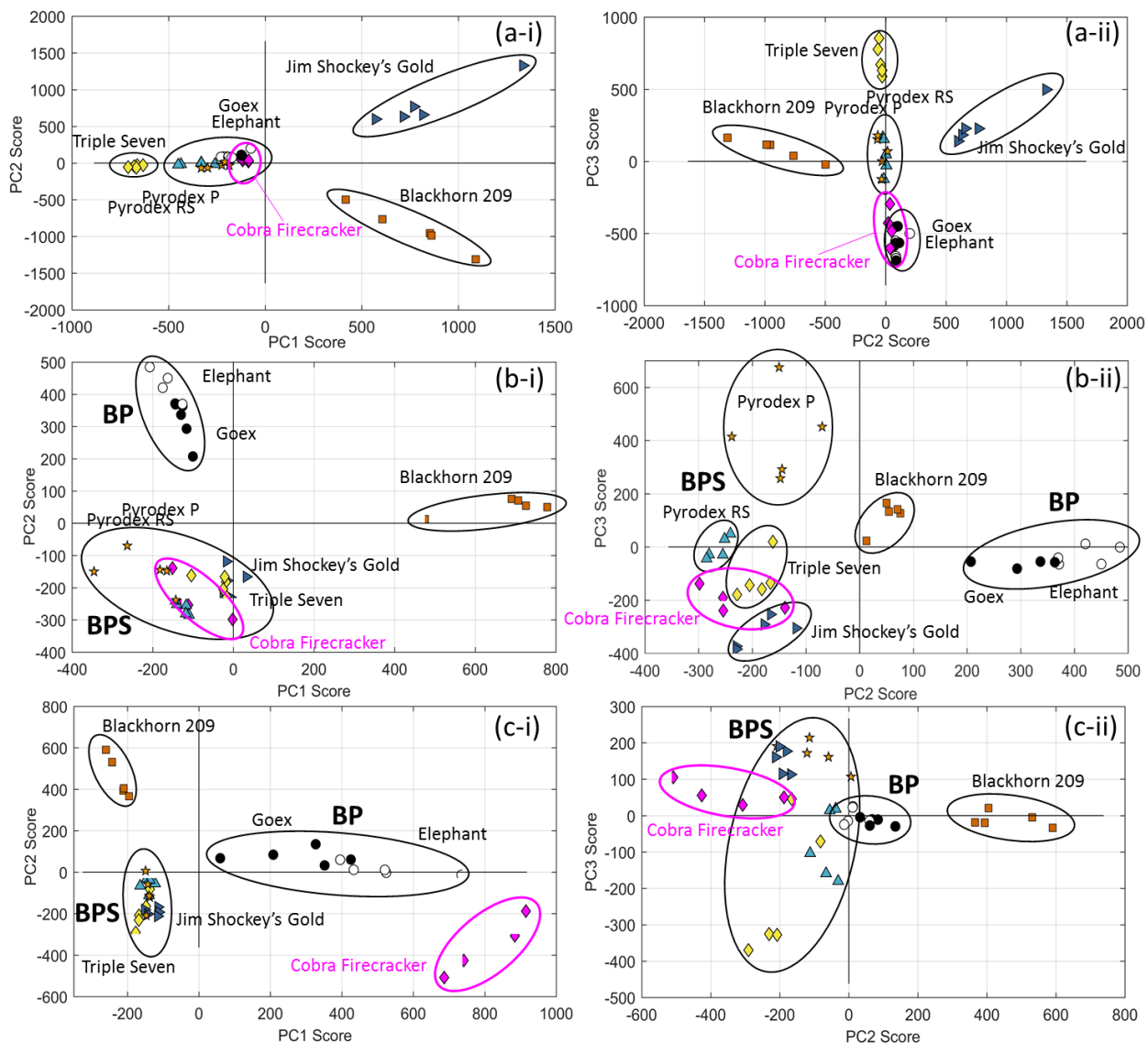


Figure S4. Principal component analysis scores plot of the mass spectral signatures (a) early and (b) late in the infrared emission interval, as well as at (c) high in-source CID. Plots display the 2D projected principal components, (i) PC1-PC2 and (ii) PC2-PC3, of the first three principal components for the training data: Elephant (○) and Goex (●) black powders, and Triple Seven (◇), Pyrodex RS (▲), Pyrodex P (★), Blackhorn 209 (■), and Jim Shockey's Gold (▶) BPS; and testing data: Cobra firecracker (◆).

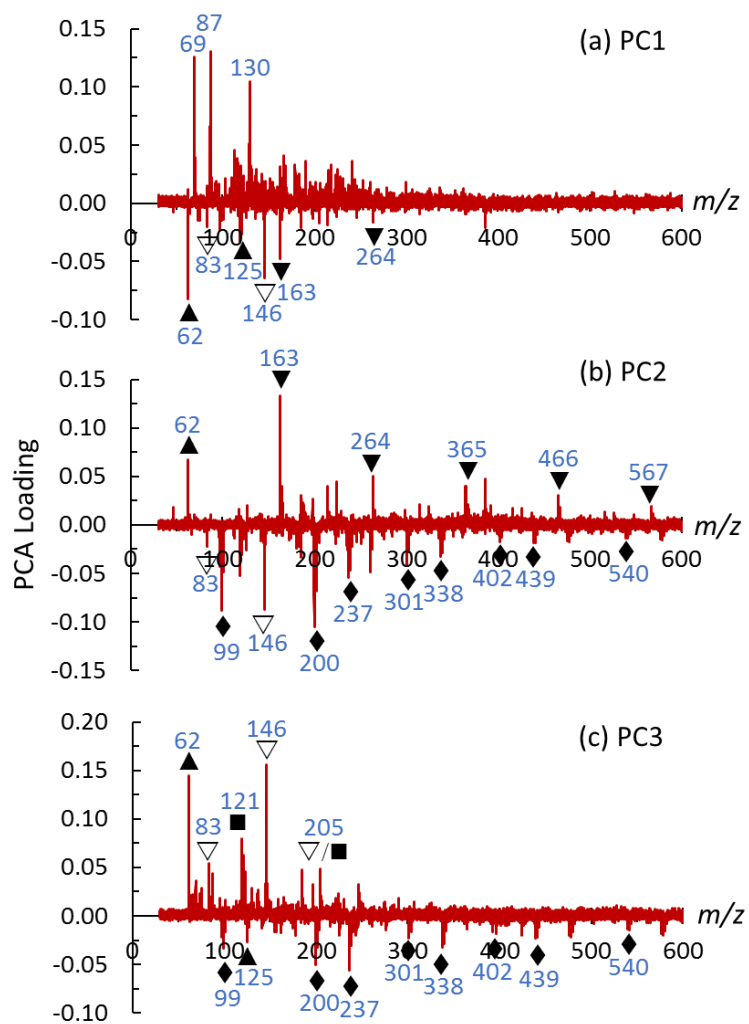


Figure S5. Principal component analysis loading plots of the mass spectral signatures late in the infrared emission interval (elevated temperatures) for the first three (a)-(c) principal components.

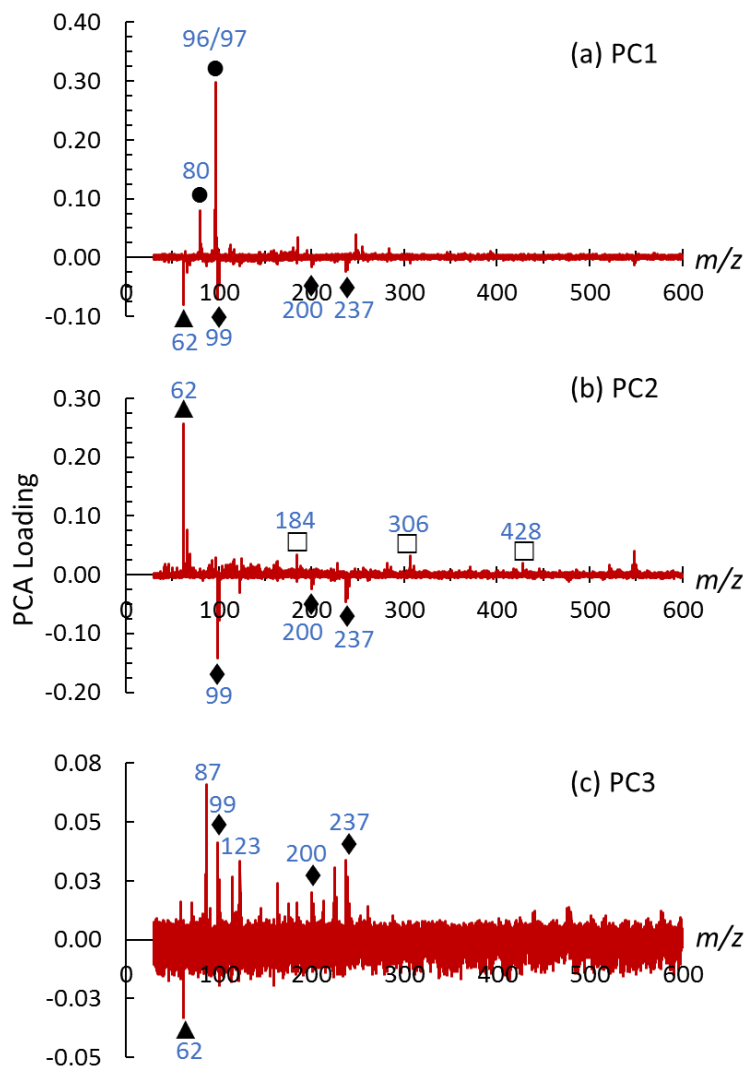


Figure S6. Principal component analysis loading plots of the mass spectral signatures at high in-source collision induced dissociation for the first three (a)-(c) principal components.

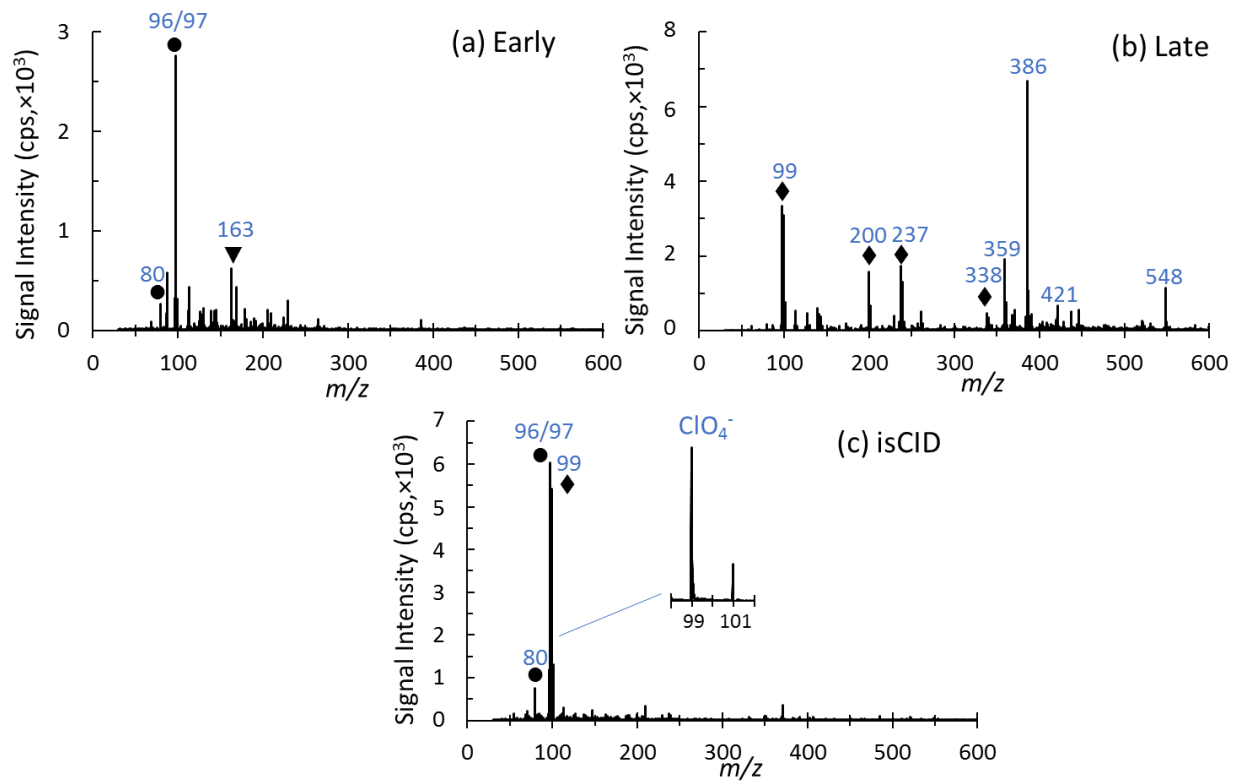


Figure S7. Representative mass spectra of Cobra firecracker from (a) early and (b) late time points during the emission interval, as well as (c) at high in-source CID. Presumptive peak identifications found in Table 1.